IChemE
www.catchword.com/titles/09603085.htm

0960–3085/02/$23.50+0.00

Trans IChemE, Vol 80, Part C, September 2002

# AN INVESTIGATION INTO THE RELATIONSHIP BETWEEN FREEZING RATE AND MEAN ICE CRYSTAL SIZE FOR COFFEE EXTRACTS

**J. M. PARDO[1], F. SUESS[2] and K. NIRANJAN[1]**

[1]*School of Food Biosciences, The University of Reading, Reading, UK*
[2]*Visiting student from Technische Universität München, Freising-Weihenstephan, Germany*

Coffee extracts—10, 20 and 40% solids content—were uni-directionally frozen. The parameters characterizing freezing kinetics, such as the rate of fall of temperature and the velocity of ice front, were determined experimentally and compared with the predictions of Neumann's model. Freeze dried samples were subsequently observed under a fluorescence microscope and the mean size of ice crystals were determined from the mean hydraulic radius of the pores. A model linking the mean hydraulic radius with freezing kinetics was developed, and the following equation was obtained: $r_H = n\exp(-mX_{so})[2\delta^2\alpha_1/s_i]^{-0.25}[(T_m - T_p)s_i^{-1}]^{-0.5}$. Here, $X_s$ is solid content, $\delta$ is Neumann's dimensionless constant, $t$ is time, $T_m$ is the initial freezing point of the extract, $T_p$ is the freezing temperature, $\alpha_1$ is the thermal diffusivity of the frozen region, $s_i$ is the position of the ice front and finally $n$ and $m$ are material related constants. Experimental data and model predictions were found to be in satisfactory agreement.

*Keywords: coffee; food; freezing; ice crystal size.*

## INTRODUCTION

A knowledge of ice crystal size distribution in frozen products is necessary in order to assess the effect of freezing on product quality. If the product is subsequently freeze dried, the drying kinetics and the quality of the dried product is also critically dependent on the ice crystal size distribution, since it influences the nature of the pores left behind by the subliming crystals[1]. Even though it is widely recognized that the ice crystal size distribution generated during freezing is critically dependent on freezing rates, there are relatively few studies that have focused quantitatively on their interrelationship, particularly for food products. This article aims to develop a model that links ice crystal size distribution with freezing kinetics for coffee extracts containing different levels of total solids.

The kinetics of freezing has been widely studied, and the determination of freezing times requires analysing conductive heat flow through frozen and unfrozen layers. The most common analyses are either based on Plank or Neumann's models which are valid for unidirectional freezing[2,3]. While Plank's model assumes quasi-steady state heat transfer, the Neumann's model is more generally applicable and is based on unsteady state conduction through frozen and unfrozen layers. Bomben and King[4] suggested the use of Plank's model to describe freezing kinetics of apple tissues and deduced a relationship between freezing rates and mean crystal size. On the other hand, Woinet *et al.*[5] have used Neumann's model to establish the link between freezing kinetics and ice crystal size for low concentration gelatin solutions (1%). Both these studies base their theories on an earlier work by Rohatgi and Adams[6] who investigated ice crystallization from dilute salt solutions. In the context of coffee extracts, there are some studies linking freezing rates with the quality of the freeze dried product, but the relationship has largely been described on a qualitative basis[7–9]. In the present study, ice crystal sizes in frozen coffee have been determined by image analysis, and linked with freezing rates described by Neumann's model.

## MATERIALS AND METHODS

### Coffee Solution

Nescafé coffee granules were used to prepare solutions of three different concentrations ($X_s = 0.1$, 0.2 and 0.4 kg solids/kg solution). The granules were dissolved in deionized water. The concentration of the samples was measured with a digital refractometer and the Brix data were converted into concentration figures using the tables reported by Sivetz and Desrosier[10]. The freezing point of each of the samples was determined by differential scanning calorimetry—peak temperature—and expressed as follows to within $\pm 0.4$°C:

$$T_m = 4.18X_s^2 - 21.03X_s, +273.15 \quad (1)$$

### Determination of Freezing Kinetics

Coffee solutions (30 g) were frozen uni-directionally in Perspex cylinders of internal diameter 50 mm. The bottom of the cylinder was fixed to an aluminium tray and the upper end was covered with an insulating cap after pouring the sample. Four thermocouples were introduced through the wall of the cylinder in order to record the temperature at

the following axial positions measured from the bottom end: 2, 7, 12 mm and the last thermocouple was positioned on the top of the cylinder with its tip covered by the liquid coffee. Due to differences in density between samples with different solute concentration, it is assumed that the positions of the last thermocouple were 16, 15 and 14 mm for the samples with solute concentration 10%, 20% and 40%, respectively. The cylinder wall was then insulated and the tray was placed in contact with a metallic surface that could be maintained at the following temperatures: $-18°C$, $-30°C$ and $-70°C$. Temperatures were recorded every minute until solidification was complete.

### Determination of Ice Crystal Size

The size of ice crystals was characterized by determining the pore size left after freeze drying the samples. The solid material, after freezing, was separated from the Perspex cylinder while maintaining its shape, and cooled to $-70°C$ using dry ice. A thin frozen layer was removed from the top in order to eliminate end effects on subsequent measurements[11]. The frozen cylindrical samples were then freeze dried in a Stokes freeze dryer at a maximum pressure of 93 Pa. Latent heat for sublimation was provided by radiation from two plates maintained below 20°C, one placed above the sample, and the other, below it. Conditions were set to avoid melting and/or collapse of the samples, therefore, the ice front temperature was maintained below $-20°C$ which has been determined as the glass transition temperature of the amorphous solid in the frozen coffee. The sample weight was recorded at regular intervals, and drying continued until no change in weight was observed over a period of at least one hour. The dried samples were subjected to image analysis.

A Zeiss fluorescence microscope (Axioscope II) fitted with a Zeiss camera (Axiocam) and image analysis software (Axiovision) was used to obtain images of the pores as viewed from the top of the cylinder. Digital images with a resolution of $1030 \times 1300$ pixels were analyzed using Scion image software (Beta 4.0.2) as shown in Figure 1. Three images from each sample were analysed. At least 150 pores were identified manually on each image; and the distribution of pore areas, $A$, and perimeters, $p_r$, were obtained. Data from all three images were normalized to give cumulative distribution parameters. The mean was taken to be the value that gave a distribution of 0.5. This procedure was repeated for three separate samples to yield the mean and standard deviation of the pore areas and perimeter. The mean pore size was characterized in terms of a hydraulic radius ($r_H$) defined as:

$$r_H = \frac{2A}{p_r} \tag{2}$$

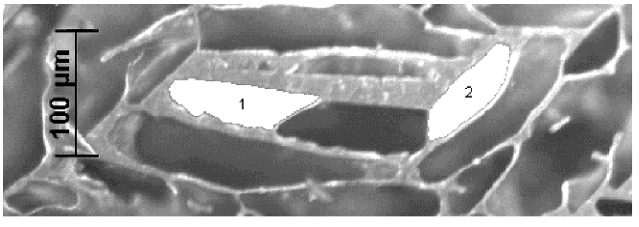


*Figure 1.* Digital image of the surface of the freeze-dried sample magnified 10×. The lightly shaded region represents amorphous solid matrix, while the darker regions represent the pores left after the sublimation of ice. Regions marked 1 and 2 represent two typical pores, which have been highlighted. The Scion image software measures the area and perimeter of such highlighted regions by counting pixels. The area of this image represents 1/20 of the total area of one microphotograph.

## RESULTS AND DISCUSSION

### Freezing Kinetics

A typical temperature profile during freezing is shown in Figure 2. The solid lines represent values estimated by Neumann's model[2], according to which, temperatures at any position in the frozen and unfrozen zones are respectively given by:

$$T_1 = T_p + (T_m - T_p)erf\left(\frac{x}{2\sqrt{\alpha_1 t}}\right) \Big/ erf(\delta) \tag{3}$$

$$T_2 = \frac{T_0}{erfc(\delta/\gamma\tilde{\alpha}^{0.5})} + (T_m - T_0)erfc \times \left\{\alpha^{-0.5}\left[\frac{x}{2\sqrt{\alpha_1 t}} + \frac{(1-\gamma)\delta}{\gamma}\right]\right\} \tag{4}$$

The thermophysical properties used in the model have been averaged over the intervals $[T_p, T_m]$ for the frozen layer and $[T_m, T_o]$ for the unfrozen layer. The methods used to estimate these properties are explained in Appendix 1. Neumann's model gives a satisfactory prediction of temperature variations, although deviations are observed below $T_m$, which are probably due to the assumption made by the model in respect of the geometry of the sample (i.e. semi-infinite) and the negligible thickness of the solidification front. It is necessary to note that Neumann's model, like any other moving boundary model, is ideal and limited in its description of a real process such as the freezing of coffee extracts. In addition to the inherent deficiency of the Neumann's model, the thermophysical properties were averaged and this could also have influenced the result to some extent. Nevertheless, the prediction of the movement of the ice front—i.e. the time at which the temperature at any axial position attains $T_m$—is more relevant to this work, and Neumann's model describes this movement satisfactorily.

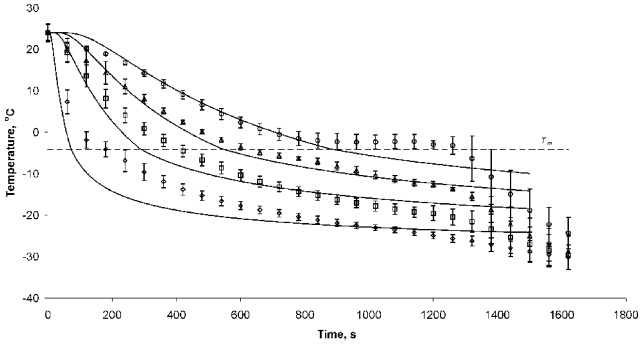


*Figure 2.* Temperature profiles at different positions upon a typical unidirectional freezing process ($x_{so} = 0.2$, $T_p = -30°C$). Axial positions measured from the bottom end of the sample: (◇) 2 mm, (□) 7 mm, (△) 12 mm (○) 15 mm. Broken horizontal line represent the initial solidification point. Solid lines represent temperature profiles calculated from Neumann's model.

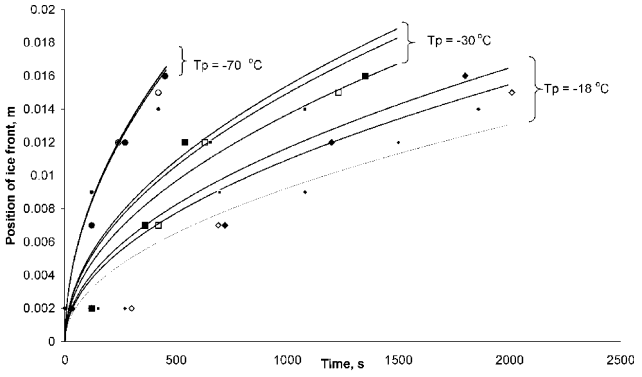


*Figure 3.* Position of ice front as a function of time: a comparison between predictions of Neumann's model and experimental data. The solid lines correspond to the estimated data from the model. In each temperature group the solid lines are organized depending on the initial solid content in the following order from top to bottom: 10%, 20% and 40%.

| Key | Solid content % | Plate temperature °C |
|---|---|---|
| ♦ | 10 | −18 |
| ◇ | 20 | −18 |
| ⬩ | 40 | −18 |
| ■ | 10 | −30 |
| □ | 20 | −30 |
| ▪ | 40 | −30 |
| ● | 10 | −70 |
| ○ | 20 | −70 |
| • | 40 | −70 |

As explained above, the movement of the freezing front can be determined using $T_m$ (see equation (1)) as an indicator. In practice, whenever a thermocouple achieved $T_m$, the position of the thermocouple was taken to be the ice front position at that instant. Figure 3 shows the experimentally determined position of the ice front reconciled against values determined by Neumann's model. According to the model, the position of the ice front is given by:

$$s_i = 2\delta\sqrt{\alpha_1 t} \tag{5}$$

where $\delta$ is a characteristic dimensionless constant obtained as a solution of:

$$\Delta H_f = \frac{C_{p1}(T_m - T_p)}{\sqrt{\pi}\delta\exp(\delta^2)erf(\delta)} - \frac{C_{p2}(T_0 - T_m)}{\sqrt{\pi}\delta/\gamma\bar{\alpha}^{0.5}\exp(\delta^2/\bar{\alpha})erfc(\delta/\bar{\alpha}^{0.5})} \tag{6}$$

Here $\Delta H_f$ is the effective latent heat of fusion, which has been corrected to account for the fraction of freezable water present in the sample (0.429 kg water/kg solids) in the following way $\Delta H_f = \Delta H_i\,(1 - 1.429X_s)$. The experimental data at all three freezing temperatures show no significant effect of coffee concentration on the movement of the ice front, although Neumann's model predicts some difference at low freezing rates. This can also be attributed to the assumption made in estimating thermophysical properties.

Tables 1 and 2 predict freezing times that are lower than those observed by 5–20%. Overall, the model under-predicts freezing time by an average of 11%. Additionally, there are discrepancies relating to the position of the ice front, especially around the top and bottom extremes of the sample. The explanation for the discrepancy observed in the bottom layers lies in the assumption that this layer freezes as soon as it makes contact with the bottom plate. With regard to the top layers, surface convection influences heat transfer despite the use of insulation, which the semi-infinite assumption of the model fails to consider.

Regardless, Figure 3 demonstrates that the Neumann's model is able to predict the rate of movement of the ice front at all times and all the freezing temperatures, especially in the range of low freezing plate temperatures. This can be further confirmed by fitting the experimental data on the transient position of the ice front to an equation of the type:

$$s_i = c_f\sqrt{t} \tag{7}$$

and comparing the values of $c_f$ with $2\delta\sqrt{\alpha_1}$ (see equation (5)). As evident in Table 1, the two values are in satisfactory agreement. The statistical validity of these results is established in Table 2.

In addition to the movement of ice front, it is also useful to compare the freezing rates ($F$) determined experimentally and from Neumann's model. Although there are different ways of defining freezing[12,13], the most appropriate definition for the purpose of this work is to regard it as the rate of change of temperature at the instant when the freezing front reaches the point where the pores are to be measured (in this case, the surface of the cylinder). In the case of unidirectional freezing, $F$, can be readily calculated using the following equation[14]:

$$F_{\exp} = \left.\frac{\mathrm{d}T}{\mathrm{d}t}\right|_{t=t_f} = RG \tag{8}$$

*Table 1.* A comparison between experimentally determined freezing kinetic parameters and the values estimated from Neumann's model.

| | | Experimental | | | | | Model | | | | |
|---|---|---|---|---|---|---|---|---|---|---|---|
| $X_s$ – | $T_p$ K | $t_f$ s | $\delta$ – | $c_f\times10^4$ $ms^{-0.5}$ | $R\times10^6$ $ms^{-1}$ | $F\times10^3$ $Ks^{-1}$ | $t_f$ s | $\delta$ – | $c_f\times10^4$ $ms^{-0.5}$ | $R\times10^6$ $ms^{-1}$ | $F\times10^3$ $Ks^{-1}$ |
| 0.10 | 255.1 | 1980 | 0.22 | 4.50 | 5.06 | 5.04 | 1883 | 0.18 | 3.69 | 4.20 | 4.18 |
| 0.10 | 243.1 | 1320 | 0.28 | 5.60 | 7.71 | 13.46 | 1077 | 0.24 | 4.88 | 7.40 | 12.92 |
| 0.10 | 203.1 | 420 | 0.43 | 8.90 | 21.71 | 92.20 | 435 | 0.37 | 7.67 | 18.00 | 76.43 |
| 0.20 | 255.1 | 2040 | 0.26 | 5.10 | 5.65 | 8.29 | 1886 | 0.18 | 3.45 | 4.00 | 5.87 |
| 0.20 | 243.1 | 1230 | 0.29 | 5.60 | 7.98 | 18.11 | 1010 | 0.25 | 4.72 | 7.40 | 16.79 |
| 0.20 | 203.1 | 420 | 0.45 | 8.90 | 21.71 | 95.50 | 374 | 0.39 | 7.75 | 20.00 | 87.96 |
| 0.40 | 255.1 | 1860 | 0.26 | 4.50 | 5.22 | 3.84 | 2294 | 0.17 | 2.92 | 3.00 | 2.21 |
| 0.40 | 243.1 | 1080 | 0.34 | 5.70 | 8.67 | 13.81 | 1048 | 0.26 | 4.32 | 6.68 | 10.64 |
| 0.40 | 203.1 | 420 | 0.47 | 8.20 | 20.01 | 89.03 | 326 | 0.45 | 7.75 | 21.50 | 95.68 |

Experimental value of $\delta$ has been estimated from $c_f\alpha_1^{-0.5}/2$.

*Table 2.* Slope and correlation coefficient for the parity plot of freezing kinetic parameters.

| | Correlation coefficient $R^2$ | Slope |
|---|---|---|
| $t_f$ | 0.93 | 0.89 |
| $c_f$ | 0.96 | 0.91 |
| $R$ | 0.96 | 0.97 |
| $\delta$ | 0.95 | 0.89 |
| $F$ | 0.98 | 1.03 |

where $R = \mathrm{d}x/\mathrm{d}t|_{x=x_i}$ and $G = (T_m - T_p)/x_i$. It is evident that $R$ represents the final rate of movement of the ice front and $G$ represents the temperature gradient of the frozen region at this instant. $R$ can be determined from the experimental data by differentiating equation (7) with respect to time and setting $t = t_f = x_i^2/c_f$. Thus, the experimental value of $R$ can be determined from the following equation:

$$R_{\text{exp}} = \frac{c_f}{2\sqrt{t_f}} = \frac{c_f^{1.5}}{2s_i} \tag{9}$$

It is also possible to determine $R$, independently, from Neumann's model by differentiating equation (5) with respect to time and setting $t = t_f = s_i^2/4\delta^2\alpha_1$. This yields:

$$R_{\text{model}} = \frac{2\delta^2\alpha_1}{s_i} \tag{10}$$

By substituting $R_{\text{exp}}$ and $R_{\text{model}}$ from equations (9) and (10) into equation (8) it is possible to determine experimental and model freezing rates, which are compared in Tables 1 and 2. It is clear from these tables that Neumann's model tends to over predict freezing times by 11% and under predict $F$ by 3%. Nevertheless, given the assumptions made in respect of the thermophysical properties, these differences are acceptable, and reinforce the use of Neumann's model to predict freezing rates defined by equation (8).

## Crystal Size

The cumulative crystal size distributions observed for different solid content and under different freezing conditions are shown in Figure 4. In Table 3 the inter-quartile range of the ice crystal size is shown for each experimental condition, which indicates the dispersion or spread of the data. The mean hydraulic radius (see equation (2)) is plotted against experimental freezing rate (equation (8)) in Figure 5. As seen from the error bars ($\pm$ one standard deviation) in this figure, the variability in the observed mean crystal size tends to increase as freezing rate decreases in the same manner as the spread in the crystal size distribution. This can be attributed to the greater influence which crystal defects have on crystal growth at lower freezing rates than at higher freezing rates[15]. Therefore, at higher freezing rates the growth tends to be more organized and the variation in the mean crystal size is lower. It is clear from Figure 5 that experimental data can be correlated as follows:

$$r_H = c_1 F^{c_2} \tag{11}$$

where $c_1$ and $c_2$ are values that appear to be influenced by the solute concentration. Values of $c_1$ are found to vary in the interval $[1.7 \times 10^{-6}, 1.2 \times 10^{-5}]$, and those of $c_2$ vary over a narrow range $[-0.23, -0.32]$ under the authors experimental conditions. The usefulness of these constants is limited, unless they are related to a more fundamental model.

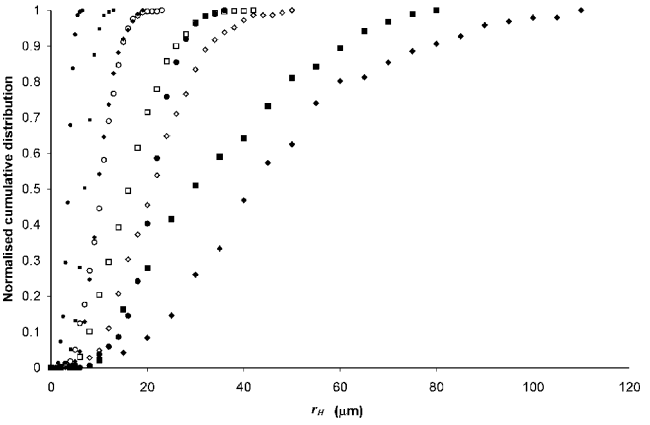


*Figure 4.* Cumulative crystal size distribution under different processing conditions.

| Key | Solid content % | Plate temperature °C |
|---|---|---|
| ♦ | 10 | −18 |
| ◇ | 20 | −18 |
| ⬩ | 40 | −18 |
| ■ | 10 | −30 |
| □ | 20 | −30 |
| ▪ | 40 | −30 |
| ● | 10 | −70 |
| ○ | 20 | −70 |
| • | 40 | −70 |

Earlier studies have characterized ice crystal growth during freezing in terms of a characteristic interdendritic distance, $L$, where ice dendrites are considered to be parallel needles growing opposite to the direction of heat transfer (see Figure 6)[4,6,16]. As ice crystal grows, there is a rejection of solute (coffee solids) and heat from the moving interface into the remaining unfrozen liquid. Due to this movement of solute and heat, concentration gradients and thermal gradients are created in the interdendritic region, and consequently supersaturation and supercooling occur. As heat transfer rates are normally much greater than mass transfer rates, solute diffusion tends to control the growth of the

*Table 3.* Inter-quartile ranges of the ice crystal size distribution at different processing conditions.

| $X_s$ | $T_p$ °C | $H_{r1} \times 10^5$ m | $H_{r2} \times 10^5$ m |
|---|---|---|---|
| 10 | −18.0 | 3.0 | 5.6 |
| 10 | −30.0 | 1.9 | 4.6 |
| 10 | −70.0 | 1.8 | 2.4 |
| 20 | −18.0 | 1.5 | 2.7 |
| 20 | −30.0 | 1.1 | 2.1 |
| 20 | −70.0 | 0.8 | 1.3 |
| 40 | −18.0 | 0.8 | 1.2 |
| 40 | −30.0 | 0.6 | 0.8 |
| 40 | −70.0 | 0.3 | 0.4 |

$H_{r1}$ and $H_{r2}$ are the lower and upper limits of the inter-quartile range, and correspond to the normalized cumulative distribution values of 0.25 and 0.75 respectively.

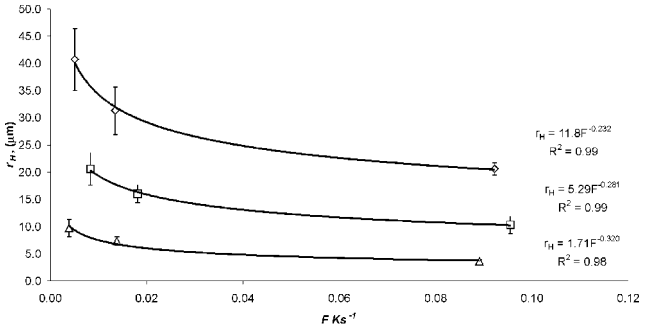


*Figure 5.* The variation of mean pore hydraulic radius (indicating ice crystal size) with freezing rate. (◇) 10% solids, (□) 20% solids, (△) 40% solids. The solid lines represent best fit curves of the form given by equation (11).

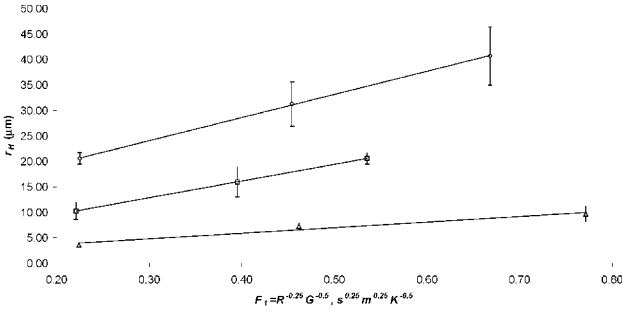


*Figure 7.* The variation of mean hydraulic radius of pores with $F_1 = R^{-0.25}G^{-0.5}$. (◇) 10% solids, (□) 20% solids, (△) 40% solids.

ice crystal. On the basis of this supercooling, theoretical equations to describe the interdendritic spacing have been proposed. Using a criterion known as growth at the extremum (i.e. minimum undercooling and maximum ice front velocity. Rohatgi and Adams[6] have theoretically shown, using Fick's second law, that in very dilute solutions, $L = (8D\Delta T_0)^{0.5}F^{-0.5}$. Given that $L \approx 2r_H$ in such solutions, it can be concluded that Rohatgi's and Adams' theory postulates:

$$r_H = (2D\Delta T_0)^{0.5}F^{-0.5} \tag{12}$$

Bomben and King[4] and Woinet *et al.*[5] showed that experimental data on the freezing of apple tissues and low concentration gelatin solutions, supported Rohatgi's and Adams' theory.

According to Kurz and Fischer[14], dendrite morphology is defined by sinusoidal perturbations at the solid–liquid interface. The wavelength of these perturbations is dependent on *R, G* and the degree of supercooling. There exists a threshold wavelength, which leads to the formation of stable dendrites; below this wavelength, the perturbations disappear. This limit is known as the limit of morphological stability and is used to define the crystal size in relation to freezing kinetics. On the basis of this theory and assuming $R > GD\Delta T_0^{-1}k^{-1}$, Kurz and Fisher[16] showed that:

$$L = 4.3\left(\frac{\Delta T_0 D\Gamma}{k}\right)^{0.25} R^{-0.25}G^{-0.5} \tag{13}$$

where $\Delta T_O$ is the supercooling between dendrites, $D$ is the binary diffusion coefficient, $\Gamma$ is Gibbs Thompson parameter related to interfacial energy and $k$ is the partition coefficient between the liquid and solidified sample.

If the data presented in Figure 4 is examined in the light of Rohatgi's and Adams' theory (see equation (12)), it is evident that the theory does not account for the observations. First of all, the data are sensitive to coffee concentration. Moreover, the exponent on $F$ according to the theory should be $-0.5$ whereas the fit of experimental data yields values around 0.3. On the other hand, if $H_r$ is plotted against $G^{-0.5}R^{-0.25}$ (see equation (13)), a linear relationship is observed for each of the solid contents used in this work (see Figure 7). This suggests that Kurz and Fisher's theory applies better to the freezing of coffee extracts. Further, it is also possible to extend Kurz and Fisher's equation empirically to relate the hydraulic radius with freezing rate for coffee extracts of different solid contents. Since the ratio $r_H/(G^{-0.5}R^{-0.25})$ was found to decrease exponentially with solute concentration, the mean hydraulic radius can be represented as:

$$r_H = n\exp(mX_{so})R^{-0.25}G^{-0.5} \tag{14}$$

Experimental data were fitted to the above equation and the values of $n$ and $m$ were found to be $1.23 \times 10^{-4}$ and $-5.36$, respectively, with $R^2 = 0.97$. Given that $G$ and $R$ can be deduced from Neumann's model (see equation (10)), it is possible to relate the mean hydraulic radius of ice crystals with the freezing condition as follows (i.e. by combining equation (14) with equations (5) and (10)):

$$r_H = n\exp(-mX_{so})\left[\frac{2\delta^2\alpha_1}{s_i}\right]^{-0.25} \times \left[(T_m - T_p)s_i^{-1}\right]^{-0.5} \tag{15}$$

Hydraulic radii determined from equations (15) are compared with experimental data in Figure 8. On average,

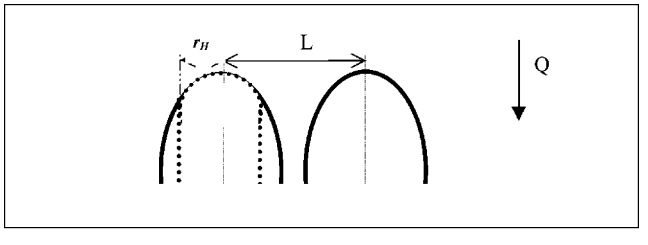


*Figure 6.* Growth of ice dendrite during freezing. $L$ is the interdendritic spacing and $H_r$ is the hydraullic radius. $Q$ represents the direction of heat transfer. For dilute solutions $L = 2H_r$.

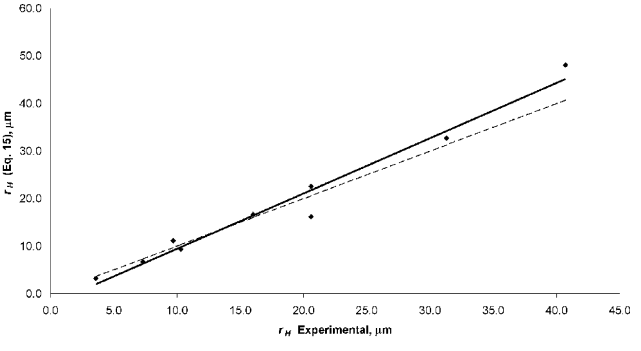


*Figure 8.* Parity plot: Mean hydraulic radius of ice crystal size, determined from equation (15) are plotted against experimental data. The broken line represents $y = x$, while the solid line is the regression line.

the model is found to over predict the mean hydraulic radius by 19%. A closer examination of this parity plot suggests that the average deviation is strongly influenced by one of the experimental conditions: 10% solute content and freezing temperature of $-18°C$, which resulted in the largest radius observed in this study. If the value corresponding to this condition in the regression analysis is neglected, then the overall difference between experimental and calculated values falls below 3% with $R^2 > 0.96$. It can, therefore, be concluded that equation (15) can be used to predict the mean hydraulic radius of ice crystals as a function of freezing conditions for coffee extracts. It is clear from equation (15) that the mean hydraulic radii are dependent on the position of the ice front. This is due to the variation of freezing rate with distance from the freezing plate, as demonstrated by the model and experimental data. However, due to the brittleness of the sample it was not possible to measure the axial variation of pore size, and this may be attempted in future.

## CONCLUDING REMARKS

(1) The movement of ice front during unidirectional freezing of coffee extracts follows the well-known Neumann's model, which satisfactorily predicts freezing rates. The model is, however, more sensitive to solid content than the experimental data appear to suggest.

(2) The mean hydraulic radius of ice crystals is proportional to $R^{-0.25}\,G^{-0.5}$ where $R$ is the final rate of movement of ice front and $G$ is the temperature gradient at this point. This proportionality is consistent with Kurz and Fisher's[16] theory for solidification of metal alloys.

(3) The following equation satisfactorily predicts the mean hydraulic radius of ice crystals formed during freezing of coffee extracts at different freezing rates: $r_H = n\exp(-mX_{so})[2\delta^2\alpha_1/s_i]^{-0.25}\left[(T_m - T_p)s_i^{-1}\right]^{-0.5}$. Here $X_{so}$ is the solid content of the coffee extract, $\delta$ is Neumann's dimensionless constant, $t$ is time, $T_m$ is the initial freezing temperature, $T_p$ is the freezing temperature and $s_i$ is the position of the ice front, finally, $n$ and $m$ which are material dependent constants take the values $1.23 \times 10^{-4}$ and 5.36 respectively for the coffee used in this study.

## APPENDIX 1

### Estimation of Thermophysical Properties

Intrinsic properties of coffee and water were used to estimate the thermo-physical of the composite sample as suggested by Woinet, Andreiu and Laurent[17]. The water was assumed to freeze at a temperature, $T_m$, given by equation (1) and the concentration of unfrozen water was taken to be 0.42 kg water/kg solid[18]. Thermophysical properties of water were obtained from Choi and Okos[19] tables and those of coffee were estimated using Costherm[20] assuming the composition of the coffee solids to be as reported by[9,21]. The thermal properties of coffee solids determined as function of temperature were expressed in the form $Y = aT^2 + bT + c$. The relevant constants are listed in Table A1. The following equations were used to calculate the composite properties of the frozen (1) and liquid (2) regions:

$$Y_1 = \varepsilon Y_s + 0.429Y_w + (1 - 1.429\varepsilon)Y_i \quad \text{(A1)}$$

$$Y_2 = \varepsilon Y_s + (1 - \varepsilon)Y_w \quad \text{(A2)}$$

where $Y$ represents either thermal conductivity or thermal difussivity. The composite heat capacity was determined as follows:

$$C_{p1} = X_s C_{ps} + 0.429X_s C_{pw} + (1 - 1.429X_x)C_{pi} \quad \text{(A3)}$$

$$C_{p2} = X_s C_{ps} + (1 - X_s)C_{pw} \quad \text{(A4)}$$

## NOMENCLATURE

| | |
|---|---|
| $A$ | area, $m^2$ |
| $C_p$ | heat capacity, $Jkg^{-1}K^{-1}$ |
| $F$ | Freezing rate, $Ks^{-1}$ |
| $F_1$ | $R^{-0.25}\,G^{-0.5}$ |
| $G$ | temperature gradient in frozen region, $Km^{-1}$ |
| $\Delta H_f$ | effective latent heat of fusion, $Jkg^{-1}$ |
| $\Delta H_i$ | ice latent heat of fusion, $Jkg^{-1}$ |
| $L$ | interdendritic spacing, $m$ |
| $L_1$ | thickness of the amorphous matrix between pores, $m$ |
| $R$ | rate of movement of ice front, $ms^{-1}$ |
| $S$ | height of the cylinder, m |
| $T$ | temperature, K |
| $T_m$ | initial freezing temperature, K |
| $X_s$ | Solid content w.b |
| | |
| $a$, $b$, $c$ | constants |
| $c_f$ | freezing kinetic empirical constant |
| $m$, $n$ | empirical constant |
| $p_r$ | pore perimeter, m |
| $r_H$ | hydraulic radius, m |
| $s$ | position of the ice front, m |
| $t$ | time, $s$ |
| $x$ | axial position coordinate, m |

*Greek Symbols*

| | |
|---|---|
| $\alpha$ | thermal diffusivity $Km^{-2}$ |
| $\bar{\alpha}$ | ratio of thermal diffusivities |
| $\alpha_2/\alpha_1$ | (liquid/frozen regions) |
| $\delta$ | Neumann's dimensionless number |
| $\varepsilon$ | volume fraction |

*Table A1*. Thermal properties of coffee solids*, water and ice** as function of temperature.

| | Thermal conductivity $Wm^{-1}K^{-1}$ | | | Thermal diffusivity $m^2s^{-1}$ | | | Heat capacity $Jkg^{-1}K^{-1}$ | | |
|---|---|---|---|---|---|---|---|---|---|
| | $a \times 10^5$ | $b \times 10^3$ | $c$ | $a \times 10^{12}$ | $b \times 10^{10}$ | $c \times 10^7$ | $a \times 10^3$ | $b \times 10^2$ | $c$ |
| Solids | 0.00 | 20.0 | 0.145 | 0.00 | 1.2 | 0.64 | 0.00 | 0.32 | 0.56 |
| Water | −0.67 | −1.9 | 0.41 | 2.4 | 19.0 | −2.2 | 5.5 | −3100 | 4.600 |
| Ice | 10.0 | −0.62 | 11.5 | 95.0 | −61.1 | 12.0 | 0.00 | 6100 | 402.4 |

*After Costherm (Jowitt *et al.*, 1983)[20]. **After Choi and Okos (1986)[19].

| | |
|---|---|
| $\gamma$ | ratio of densities, $\rho_1/\rho_2$ |
| $\rho$ | density |

*Subscripts*

| | |
|---|---|
| 1 | frozen region |
| 2 | liquid region |
| *f* | final |
| *i* | ice front |
| *o* | initial |
| *p* | freezing plate |

## REFERENCES


1. Mellor, J. D., 1978, *Fundamentals of Freeze Drying* (Academic Press, London, UK).
2. Carslaw, H. and Jaeger, J., 1959, *Conduction of Heat in Solids*, 3rd ed (Clarendon Press, Oxford, UK).
3. Özilgen, M., 1998, *Food Process Modeling and Control* (Gordon and Breach Science Publishers, Amsterdam, The Netherlands).
4. Bomben, J. and King, C., 1982, Heat and mass transport in freezing of apple tissue, *J Food Tech*, 17: 615–632.
5. Woinet, B., Andrieu, J. and Laurent, M., 1998, Experimental and theoretical study of model food freezing. Part II. Characterization and modelling of the ice crystal size, *J Food Eng*, 35: 395–407.
6. Rohatgi, P. and Adams, C., 1967, Effect of freezing rates on dendritic solidification of ice from aqueous solutions, *Trans Metal Soc, AIME*, 239: 1729–1736.
7. Petersen, E. and Loretzen, J., 1973, Influence of freeze drying parameters on the retention of flavor compounds of coffee, *J Food Sci*, 38: 119–122.
8. Flink, J., 1975, The influence of freezing conditions on the properties of dried coffee, In: *Freeze Drying and Advanced Food Technology*, Goldblith, S., Rey, L. and Rohmayr, W. (eds.) (Academic Press, London, UK), pp 143–160.
9. Clarke, R. J. and Macrae, R., 1987, *Coffee V1 Chemistry Technology* (Elsevier Applied Science, London, UK).
10. Sivetz, M. and Desrosier, N., 1979, *Coffee Technology* (The AVI Publishing Company, Conneticut, USA).
11. Sagara, Y. and Ichiba, J., 1994, Measurement of transport properties for the dried layer of coffee solutions undergoing freeze drying, *Dry Tech*, 12(5): 1081–1103.
12. International Institute of Refrigeration, 1986, *Recommendations for the Processing and Handling of Frozen Foods*, 3rd ed (Paris, France).
13. Chevalier, D., Le Bail, A. and Ghoul, M., 2000, Freezing and ice crystals formed in a cylindrical Food model: Part I. freezing at atmospheric pressure, *J Food Eng*, 46: 277–285.
14. Kurz, W. and Fisher, D., 1987, *Fundamental of Solidification* (Trans Tech Publications, Germany).
15. Sahgian, M. and Douglas, G., 1995, Fundamental aspects of the freezing process, *Freezing Effects on Food Quality* (Marcel Dekker, New York, USA).
16. Kurz, W. and Fisher, D. J., 1981, Dendrite growth at the limit of stability: Tip radius and spacing, *Acta Metallurgica*, 29: 11–20.
17. Woinet, B., Andrieu, J. and Laurent, M., 1998, Experimental and theoretical study of model food freezing. Part I. Heat transfer modeling, *J Food Eng*, 35: 381–393.
18. Nakamura, K., Kumagai, H. and Yano, T., 1986, Effect of freezing conditions on freeze drying rate of concentrated liquid foods, *Food Eng and Proc App* (Elsevier Applied Science, London, UK), Vol 1, pp 443–450.
19. Choi, Y. and Okos, M., 1986, Effect of temperature and composition on thermal properties of foods, *Food Eng and Proc App* (Elsevier Applied Science, London, UK), Vol 1, pp 93–101.
20. Jowitt, R., Escher, F., Hallstrom, B., Meffert, H. F., Spiess, W. E. L. and Vos, G., 1983, *Physical Properties of Foods* (Elsevier Applied Science, London, UK), Vol 1.
21. Illi, A. and Viani, R., 1995, *Espresso Coffee: The Chemistry of Quality* (Academic Press, London, UK).


## ACKNOWLEDGEMENTS

The support of America Latina Formación Académica (ALFA) programme, established between The University of Reading (UK) and La Universidad de La Sabana (Colombia), is gratefully acknowledged. The authors would also like to express their gratitude to Mr Stefan Padar for his help in the experimental study.

## ADDRESS

Correspondence concerning this paper should be addressed to Dr K. Niranjan, School of Food Biosciences, University of Reading, PO Box 226, Whiteknights, Reading RG6 6AP, UK.
E-mail: afsniran@reading.ac.uk

*The manuscript was received 11 July 2001 and accepted for publication after revision 23 April 2002.*